

## RESEARCH ARTICLE

# Proteomic exploration of the impacts of pomegranate fruit juice on the global gene expression of prostate cancer cell

Song-Tay Lee, Yi-Ling Wu, Lan-Hsiang Chien, Szu-Ting Chen, Yu-Kai Tzeng and Ting-Feng Wu

Department of Biotechnology, Southern Taiwan University of Science and Technology, Tainan, Taiwan

Prostate cancer has been known to be the second highest cause of death in cancer among men. Pomegranate is rich in polyphenols with the potent antioxidant activity and inhibits cell proliferation, invasion, and promotes apoptosis in various cancer cells. This study demonstrated that pomegranate fruit juice could effectively hinder the proliferation of human prostate cancer DU145 cell. The results of apoptotic analyses implicated that fruit juice might trigger the apoptosis in DU145 cells via death receptor signaling and mitochondrial damage pathway. In this study, we exploited 2DE-based proteomics to compare nine pairs of the proteome maps collected from untreated and treated DU145 cells to identify the differentially expressed proteins. Comparative proteomics indicated that 11 proteins were deregulated in affected DU145 cells with three upregulated and eight downregulated proteins. These dys-regulated proteins participated in cytoskeletal functions, antiapoptosis, proteasome activity, NF- $\kappa$ B signaling, cancer cell proliferation, invasion, and angiogenesis. Western immunoblotting were implemented to confirm the deregulated proteins and the downstream signaling proteins. The analytical results of this study help to provide insight into the molecular mechanism of inducing prostate cancer cell apoptosis by pomegranate fruit juice and to develop a novel mechanism-based chemopreventive strategy for prostate cancer.

Received: February 27, 2012

Revised: July 12, 2012

Accepted: August 14, 2012

**Keywords:**

Apoptosis / Biomedicine / ENO1 / Pomegranate / Prostate cancer

## 1 Introduction

Prostate cancer (CaP) is known to be the most common malignancy in men and the second leading cause of cancer mortalities among US males with a similar trend in many Western

countries and in Taiwan [1, 2]. Adenocarcinoma is responsible for 95% of prostatic neoplasms, despite the usual lack of specific presenting symptoms. This cancer usually develops in men over the age of 50. There are about 15–30% cases of mortality among those diagnosed with prostate cancer [2, 3]. Many epidemiologic and basic science reports strongly implicate that plant-derived phytochemicals may play an essential role in prostate cancer prevention or treatment [4–7]. Epidemiologic studies show that a risk of prostate cancer can be reduced by the consumption of fruits and vegetables rich in phytochemicals including hydrolyzable tannins (ellagitannins and gallotannins), condensed tannins (proanthocyanidins), anthocyanins, and other flavonoids [8].

Pomegranate (*Punica granatum*, Punicaceae), is an edible fruit cultivated in Mediterranean countries, Afghanistan, India, China, Japan, Russia, the United States, and few in Taiwan. Edible portions (80% of total fruit weight)

**Correspondence:** Dr. Ting-Feng Wu, Department of Biotechnology, Southern Taiwan University of Technology, 1 Nan-Tai Street, YungKang District, Tainan 701, Taiwan

**E-mail:** wutingfe@mail.stut.edu.tw

**Fax:** +886-6-242-5741

**Abbreviations:** **ARP2**, actin-related protein 2 homolog; **CaP**, prostate cancer; **ENO1**,  $\alpha$ -enolase; **HIF-1 $\alpha$** , hypoxia-inducible factor 1- $\alpha$ ; **HSC**, human hepatic stellate cells; **JNK**, c-jun N-terminal kinase; **LMNA**, lamin A/C; **PE**, pomegranate extract; **PFE**, pomegranate fruit extract; **PFJ**, pomegranate juice; **PI**, propidium iodide; **PSMA3**, proteasome subunit  $\alpha$  type 3; **Rb**, retinoblastoma protein; **TCTP**, translationally controlled tumor protein; **UBE2N**, ubiquitin conjugating enzyme E2N; **VCP**, valosin containing protein; **VEGF**, vascular endothelial growth factor

**Colour Online:** See the article online to view Fig. 3 in colour.

of pomegranate fruit comprise 80% juice and 20% seed. Pomegranate contains crude fibers, pectin, sugars, and polyphenols [tannins (mainly ellagitannins), flavonoids, and anthocyanins] that provide the fruit potent antioxidant activity [9–12].

Many well-documented evidences have showed that pomegranate fruit possesses anti-cancer potential. Anthocyanin/ellagitannin-rich pomegranate fruit extract (PFE) product isolated from pomegranate edible portion with 70% acetone was found to revert the apoptotic effects on human lung cancer A549 cells by the down-regulation of cell-cycle regulatory proteins operative in the G<sub>1</sub> stage and inhibiting NF- $\kappa$ B as well as Map kinase pathway (p38, PI3K/Akt, JNK, and Erk) [13]. In primary lung tumor animal model, PFE also diminishes tumor growth/progression/angiogenesis by the suppression of NF- $\kappa$ B, Map kinase pathway (p38, PI3K/Akt, JNK, and Erk) and mTOR signaling [14]. In addition to the impacts on lung cancer, various preparations of pomegranate were examined on human prostate cancer. Oral feeding of 0.1% and 0.2% w/v PFE significantly retards the tumor growth of androgen-responsive CWR22Rv1 cell in athymic nude mice. It can cause G<sub>1</sub>-phase arrest and induce PC3 cell apoptosis. The induction of G<sub>1</sub> phase arrest and cell apoptosis is invoked by overexpression of proapoptotic Bax and Bak, downregulation of antiapoptotic Bcl-1 and Bcl-XL, an increase in WAF1/p21 and KIP1/p27, dwindling in cyclins D and E and a decrease in cyclin-dependent kinase-2, -4, and -6 [15]. Other investigations on prostate cancer found that pomegranate extract (PE) product made from fruit skins standardized to ellagitannins can restraint prostate cancer cell possibly caused by chronic inflammation via suppressing NF- $\kappa$ B pathway, which is well-established signaling pathway mediating the inflammation relevant to cancer [16]. Prostate cancer initially occurs as an androgen-dependent lesion; however, advanced tumor acquires the androgen-independence. Hong et al. [17] reported that pomegranate polyphenols, ellagitannin-rich extract can reduce the gene expressions of key androgen-synthesizing enzymes, suggesting that inhibition of androgen-synthesizing enzymes by pomegranate polyphenols may be of particular importance in androgen-independent CaP cells. PE was also observed to inhibit angiogenesis in prostate cancer through downregulation of hypoxia-inducible factor 1- $\alpha$  (HIF-1 $\alpha$ ) that controls the expression of vascular endothelial growth factor (VEGF) by transcriptional regulation [18]. Tumor-induced angiogenesis is controlled by VEGF and the VEGF levels are elevated in prostate cancer both in animal model and human [19]. Owing to the potent antioxidant activities, pomegranate also exhibits the abilities of antiinflammation [20] and hepatoprotection [21].

In this study, we used 2DE coupled with MS/MS to explore the molecular mechanism underlying the cancer intervention of pomegranate juice (PFJ). We found that pomegranate fruit can dampen prostate cancer via inhibiting the expression of genes linked to apoptosis, metabolic transformation (en-

ergy production), ubiquitin/proteasome degradation, NF $\kappa$ B signaling pathway, invasion/metastasis, angiogenesis, and cytoskeleton.

## 2 Materials and methods

### 2.1 Preparation of pomegranate fruit juice

Hundred percent PFJ (Royal Chef Brand) imported from Republic of Georgia by Sky Chefs International, Inc. was purchased for the experiments. The PFJ was frozen, dried, and prepared as a 250- $\mu$ g/ $\mu$ L stock solution in sterile water and named as PFJ.

### 2.2 IEF and SDS-PAGE

2DE was carried out as described before with some modifications [22]. The pH 4–7, 18-cm immobililine dry strips (GE Healthcare Bio-Sciences AB, Uppsala, Sweden) were rehydrated for 16 h at 20°C with 300  $\mu$ L rehydration buffer containing 100  $\mu$ g protein lysates prepared from each of PFJ-exposed and unexposed DU145 cells using BioRad Protean IEF Cell. The proteins were then focused at 20°C at 50V, 100V, 200 V, 500 V, 1000 V, 5000 V, and 8000 V, respectively with a total of 81 434 voltage-hours. After equilibrated in equilibration buffer containing 2% w/v DTT and in equilibration buffer containing 5% w/v iodoacetamide, the equilibrated gel was loaded onto the top of a 12.5% w/v polyacrylamide gel and the proteins were separated at 420 V using BioRad Protean Ixi.

### 2.3 Silver staining and image analysis

The silver staining was performed as described elsewhere [22]. Glutardialdehyde was not used in the silver staining due to the protein identification by MS. The images of 2DE gel map were captured using BioRad GS800 Densitometer (Bio-Rad Laboratory, Hercules, CA). To search for the deregulated proteins in PFJ-exposed DU145 cells, a total of nine pairs of well-focused gel maps collected from control and PFJ-incubated DU145 cells were compared by PDQuest 8.0.1 (BioRad) software. Dys-regulated expressed protein spots identified by computer analysis were further confirmed by visualization. The intensity of the spot was measured and normalized as a percentage of the total intensities of all spots in a gel and analyzed with Student's *t*-test (STATISTICA, StatSoft, Tulsa, OK, USA). For each differentially expressed protein spot volumes of individual protein spots across replica gels of naive or PFJ-exposed DU145 cells were analyzed by the normal distribution test and then Student's *t*-test was carried out when the normal distribution was obtained. However, when the normal distribution was not acquired, log transformation was performed followed by the normal distribution

test and Student's *t*-test. In all cases, statistical variance of the PFJ treated: control spot intensity ratio within 95% (Student's *t*-test;  $p < 0.05$ ) was considered to be significantly different. Furthermore the differentially expressed proteins present at least in five of nine gel pairs were regarded as PFJ-influenced proteins.

## 2.4 In-gel digestion and protein identification analysis via LC-MS/MS

The in-gel digestion and mass spectrometric analysis were performed as described previously [22]. Briefly, the protein digest was separated in LTQ-Orbitrap hybrid tandem mass spectrometer (ThermoFisher, USA) in-line coupled with Agilent 1200 nanoflow HPLC system equipped with LC Packing C18 PepMap 100 (length: 5 mm; internal diameter: 300  $\mu$ m; bead size: 5  $\mu$ m) as the trap column and Agilent ZORBAX XDB-C18 (length: 50 mm; internal diameter: 75  $\mu$ m; bead size: 3.5  $\mu$ m) as the separating column. File Converter in Xcalibur 2.0SR package (ThermoFisher, USA) and an in-house program were used to extract the MS/MS information as well as to compute the charge and mass for each analyzed peptide. TurboSequest program (ver. 27, rev. 11) was then used to search the best matched peptides from a nonredundant protein database whose FASTA sequences were downloaded from National Center for Biotechnology Information (<ftp://ftp.ncbi.nlm.nih.gov/pub/nonredundant/>) on 5th May 2008 with 440 000 entries. While only the tryptic peptides with 2 or more missed cuts were considered, the mass ranges during the database search were 1 and 3.5  $m/z$  for fragment and precursor ions, respectively. The protein identities were verified only when there were at least two peptides matched and both search results had high Xcore (i.e.  $\geq 2.0$  for doubly charged peptides and  $\geq 3.0$  for triply charged ones) and with minimal differences between observed and hypothetical masses (i.e.  $\Delta M < 10$  ppm). For each set of MS/MS analyses, 25 fmol of BSA in gel was analyzed in parallel for verification of effectiveness of the entire protein identification procedure, including in-gel digestion, nanoflow HPLC, MS/MS, and informatics analyses. The experimental data were only taken into account only when 10 ppm mass accuracy and over 70% coverage was observed for the coprocessed BSA sample.

## 2.5 Western immunoblotting

After treatment as described in Section 3, DU145 cells were harvested and lysed in lysis buffer [10 mM Tris (pH 8.0), 0.32 M sucrose, 1% v/v Triton X-100, 5 mM EDTA, 2 mM DTT, and 1 mM PMSF]. After determining its protein concentration using Bio-Rad DC protein assay kit, equal volume of 2  $\times$  sample buffer [0.1 M Tris (pH 6.8), 2% SDS, 0.2%  $\beta$ -mercaptoethanol, 10% v/v glycerol, and 0.0016% w/v bromophenol blue] was combined with the cytoplasmic extract. Appropriate amounts of the lysates were separated by electrophoresis at 100 V with

10% w/v SDS-PAGE, and further transferred on to a PVDF membrane (Stratagene, La Jolla, CA, USA). After blocking for 1 h in 3% (w/v) bovine albumin serum (BSA) at room temperature, membranes were hybridized overnight at 4°C with primary antibodies against valosin containing protein (Abnova, Taipei, Taiwan),  $\alpha$ -enolase (Abnova), lamin A/C (Abnova), GAPDH (Abnova),  $\beta$ -actin (Spring Bioscience, CA, USA), NF- $\kappa$ B (p65) (Enzo, NY, USA), and phospho-c-Jun N-terminal kinase (Cell signaling, Danvers, MA, USA). The membranes were washed and probed with suitable secondary antibodies for 1 h at room temperature. Secondary antibodies binding on the membrane were detected by chemiluminescence ECL detection system (Amersham-Pharmacia Biotech Inc., Piscataway, NJ, USA) using Fujifilm LAS-3000 Luminescent Image Analyzer (Fujifilm Corporation, Tokyo, Japan). The intensity of each protein band was quantified by PDQUEST Quantity One software (Bio-Rad Laboratory) and normalized with GAPDH protein expression level.

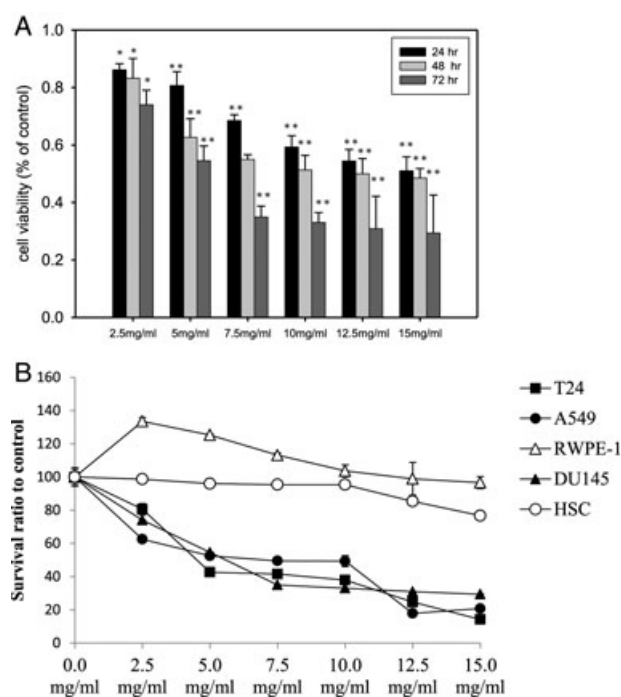


**Figure 1.** The inhibitory influences of PFJ on DU145 cells. (A) DU145 cells were incubated with the indicated amounts of PFJ for 24, 48 as well as 72 h and cell viability was measured by MTT assay as described in Section 2. \* and \*\* represented  $p < 0.05$  and  $p < 0.001$ , respectively as compared to untreated cell using Student's *t*-test. The diagram was the typical result of three independent experiments. (B) The selectivity of PFJ was determined by dose-dependent response against HSC, RWPE-1, T24, A549, and DU145 cells carried out by exposing the cells in the presence of the indicated concentrations for 72 h. The figure was the representative data of three independent examinations. All the data were expressed as mean  $\pm$  SD of the mean of four wells.

For detecting lamin A/C, DU145 cells were lysed in 1 × sample buffer [0.5 M Tris (pH 6.8), 1% w/v SDS, 0.1% v/v β-mercaptoethanol, 5% v/v glycerol] and total cell lysates were analyzed as described above.

### 3 Results

#### 3.1 Inhibitory effects of PFJ on outgrowth of human DU145 prostate cancer cell

In many well-documented studies, various extracts isolated from pomegranate fruit juice are exploited for investigating the apoptotic effects of pomegranate on prostate cancer. However, in this study the commercially available pomegranate fruit juice was implemented to demonstrate the apoptotic effect on prostate cancer. Thus, to examine whether PFJ had the inhibitory effects on DU145 cells, DU145 cells were incubated for different time durations (0–72 h) with or without various concentrations of PFJ (2.5–12.5 mg/mL). The experimental results in Fig. 1A demonstrated that the impact of PFJ could be noticed after treatment for 24 h with 10 mg/mL. The suppressive effects of PFJ were more prominent after treatment for 72 h with more than 5 mg/mL. After 72 h, approximately 70% of DU145 cells were dead after incubation with more than 7.5 mg/mL of PFJ. The observation results implied that PFJ influenced the viability of DU145 cells in a time- and dose-dependent manner (Fig. 1A).

The inhibitory influence of PFJ on cell survival observed in DU145 cells implicated that PFJ might similarly affect normal cells. Human hepatic stellate cells (HSC) and RWPE-1 cells were employed to investigate this possibility. As indicated in Fig. 1B, virtually almost all the HSC and RWPE-1 cells survived after 72 h treatment with all the PFJ concentrations tested. However, PFJ could hinder bladder cancer T24 cell, lung cancer A549 cell, and DU145 cell in a dose-dependent manner with similar inhibitory activity. Thus normal and cancer cell lines exhibited differential sensitivity to PFJ.

#### 3.2 PFJ impeded survival of human DU145 cells by triggering apoptosis

According to the above results, PFJ could invoke an inhibitory impact on DU145 cell survival. However, necrosis or apoptosis may be associated with the killing of DU145 cells by PFJ. To discover which mechanism was involved in the killing of DU145 cells, PFJ-treated DU145 cells were examined with the subG<sub>1</sub> cell analysis and annexin V/PI staining using flow cytometry. Flow cytometric analyses demonstrated that each of the PFJ concentrations under study (5, 7.5, 10, and 12.5 mg/mL) could induce the formation of prominent hypodiploid subG<sub>1</sub> peak after incubation for 72 h (Fig. 2A), reflecting that PFJ could cause the DNA fragmentation in DU145 cells, which is a typical phenomena of late apoptotic cell. The distribution of G<sub>0</sub>/G<sub>1</sub>, S, and G<sub>2</sub>/M phases of

PFJ-treated DU145 cells was showed in Supporting Information Table S1. Besides, the results of annexin V/PI staining showed that after incubation for 72 h 12.5 mg/mL of PFJ could induce the phosphatidylserine translocation in the cell membrane, which is an initial sign of apoptosis and causes the subsequent membrane leakage (late apoptotic cell) and thus increase the percents of early and late apoptotic cells (Fig. 2B).

#### 3.3 PFJ caused apoptosis in DU145 cell by evoking the mitochondrial pathway and death receptor signaling

The results of flow cytometry demonstrated that PFJ might induce the apoptosis in DU145 cells. However, cytometric analysis cannot uncover whether PFJ leads to the apoptosis by death receptor signaling, mitochondrial damage pathway, or ER stress. To explore the mechanism by which PFJ invoked the apoptosis, the processing and activation of caspase-3, which is considered to play a central role in death receptor signaling and mitochondrial damage and can be activated by caspase-8 in death receptor signaling as well as by caspase-9 in mitochondrial damage, was examined by the caspase-3 activity assay and western blotting. As shown in Fig. 2C, the activity of caspase-3 was increased temporally in 12.5 mg/mL PFJ-exposed DU145 cells and the amount of pro-caspase-3 was also dwindled in a time-dependent manner, implying that caspase-3 was activated and the apoptosis might be initiated via mitochondrial damage or death receptor signaling. To further clarify the apoptotic mechanism mediated by PFJ, the activities of caspase-8 and -9 in PFJ-treated DU145 cells was examined by the activity assay. The data in Fig. 2 showed that the activities of caspase-8 and -9 were augmented in 12.5 mg/mL PFJ-administrated DU145 cells in a time-dependent manner, and Western immunoblotting demonstrated that the quantities of procaspase-9 was decreased temporally, suggesting that PFJ could induce DU145 cell apoptosis through the mitochondrial pathway and death receptor signaling.

#### 3.4 2DE of PFJ-treated DU145 cells

Based on the data presented above, PFJ may initiate a cascade of biochemical events to induce DU145 cell apoptosis. To elucidate these events, 2DE coupled with MS was conducted to profile protein expression and search for proteins whose expressions were altered by PFJ incubation. DU145 cells were treated for 24 h with or without 7.5 mg/mL PFJ. A 7.5 mg/mL treatment was selected because, as indicated by the results shown by Fig. 1, sufficient affected cells that were at the same time still viable could be collected and potentially relevant cellular changes prior to cell death could typically be observed in DU145 cells treated with 7.5 mg/mL PFJ after 24 h, a concentration that is effective and selective to impede survival of cancer but not normal cells. Initially, 100 μg of

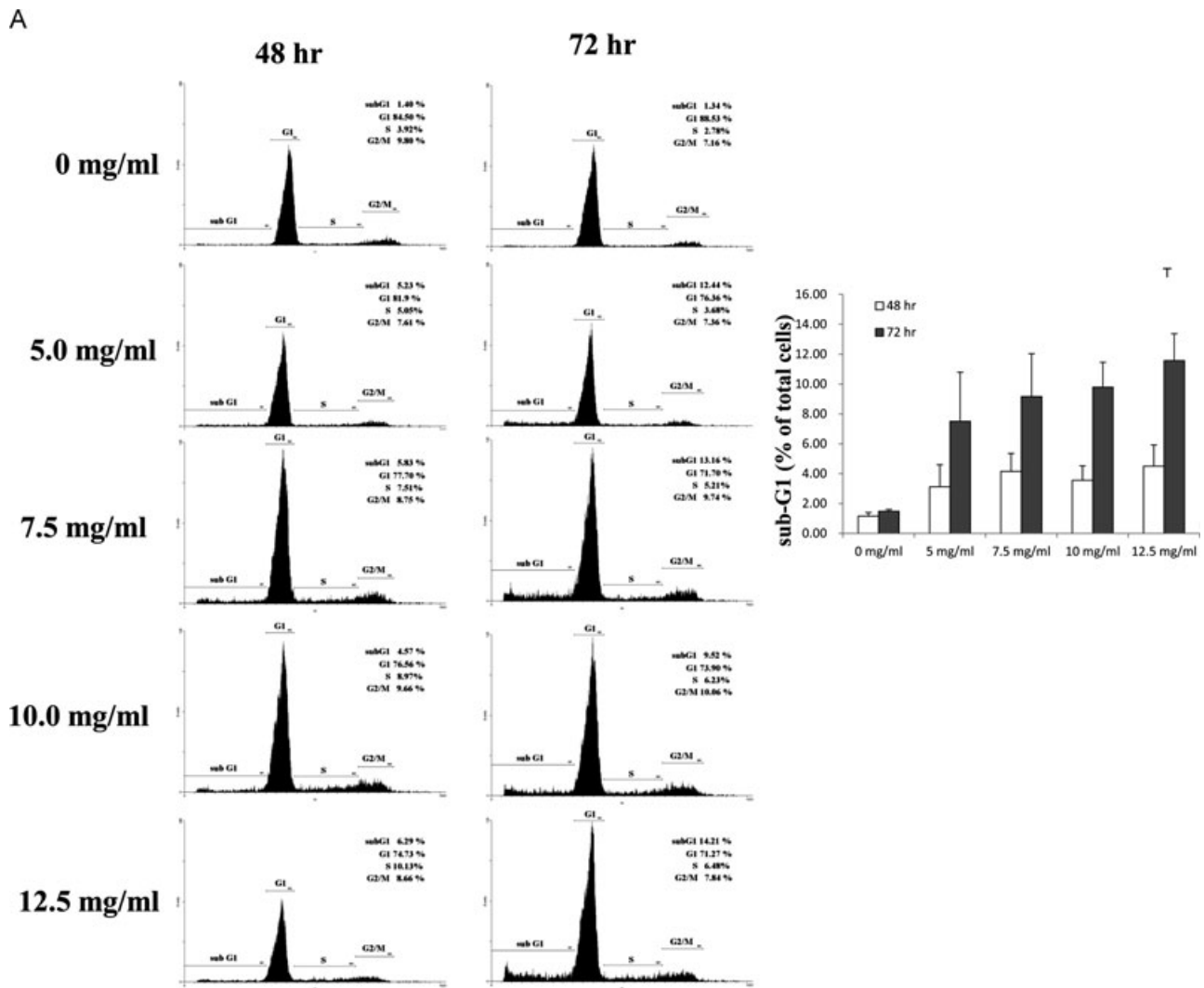


**Figure 2.** Induction of DU145 cell apoptosis by PFJ. (A) DU145 cells were incubated with the indicated amounts of PFJ for 48 as well as 72 h and sub-G<sub>1</sub> analyses were determined by flow cytometry as described in the Supporting Information data. The figure was the representative result of three independent experiments and the mean  $\pm$  SD was indicated in right panel. (B) Apoptotic effect was also observed by treating DU145 cells with 12.5 mg/mL of PFJ for 24, 48 as well as 72 h and the effect was measured by the Annexin V/PI staining as described in the Supporting Information data. The diagram was the representative data of three independent experiments and the mean  $\pm$  SD was demonstrated in lower panels. Control cell was the untreated DU145 cell. (C) DU145 cells were treated with 12.5 mg/mL PFJ for 24, 48, and 72 h. The caspase-3, -8, and -9 activities were measured by colorimetric assay kit as described in the Supporting Information data. The activity assays were performed in three independent experiments. \* indicated  $P < 0.05$  as compared to control cell using Student's *t*-test. (D) DU145 cells were treated with 12.5 mg/mL PFJ for 0, 24, and 48 h. Western immunoblotting was carried out to detect the depression of pro-caspase-3 and -9 production, indicating that procaspase-3 and -9 were degraded to produce the activated caspases. The blot was the typical result of three independent experiments.

proteins from control and PFJ-incubated DU145 cells were loaded and separated by 2DE of 18-cm gel strips (pI 4–7). To prevent the variation of silver staining, nine replicate gel pairs were gathered from three independent experiments. The representative 2DE maps of control and PFJ-exposed DU145 cells are depicted in Fig. 3. Each gel resolved up to approximately 850 protein spots. The other gel pairs were shown in the Supporting Information Fig. S1.

The proteome maps of control and PFJ-administrated DU145 cells were compared with PDQUEST software to identify the protein spot variations. After PFJ treatment, differentially expressed protein features were recorded, which were higher than twofold in magnitude as observed in at least five of nine replica gel pairs and statistically significant. Eight down-regulated and three upregulated protein spots were found as denoted by the arrowed spots in Fig. 3. Spots 2 and 3 were

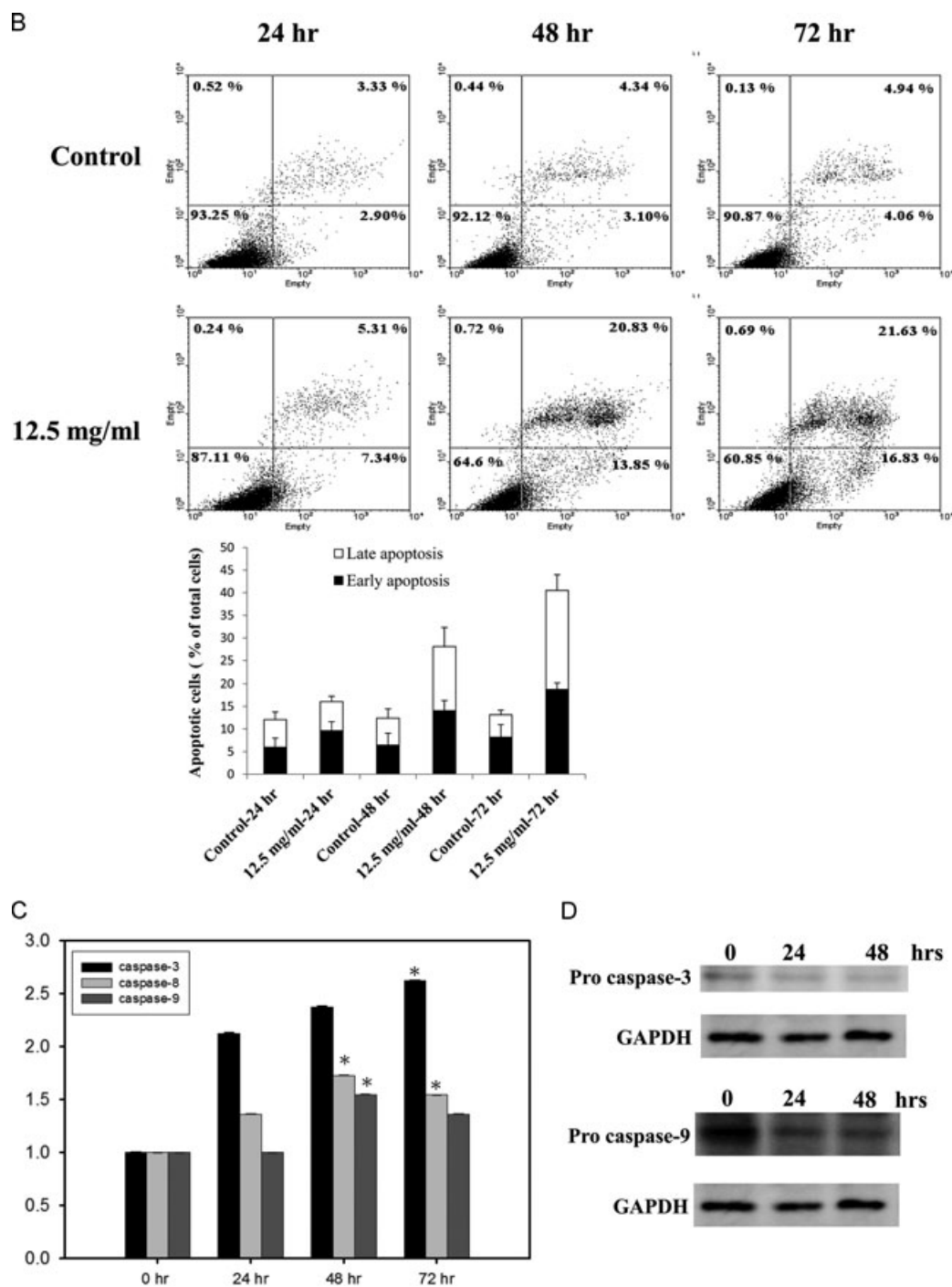
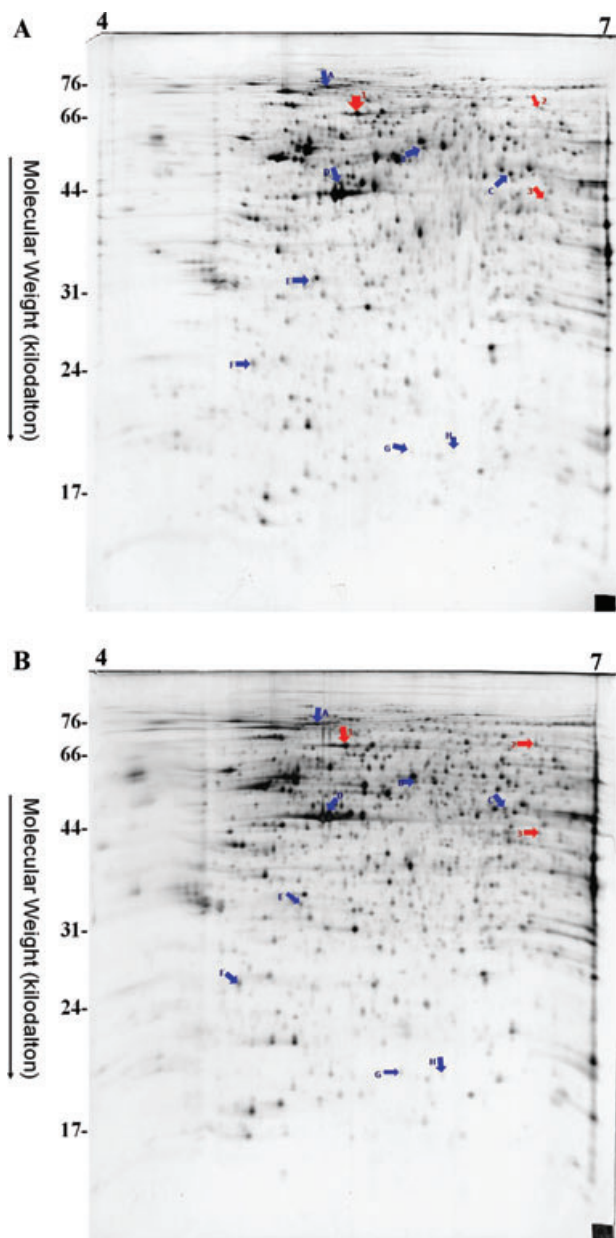


Figure 2. Continued.

over twofold but close to statistical significant while spot A was not statistical significant. The total normalized volume [volume (ppm)] and statistical result of each protein spot are presented in Supporting Information Table S2. The total normalized volume was evaluated by the intensity of each spot divided by the sum of intensities of all spots in the gel.

### 3.5 Identification of differentially expressed proteins in PFJ-impacted DU145 cells

After analyzing the proteome maps, peptides were extracted from each differentially expressed protein spot by in-gel tryptic digestion and proteins were identified using tandem



**Figure 3.** Silver stained 2DE polyacrylamide gels of untreated and PFJ treated in pH ranges 4–7. Protein lysates were prepared from 7.5 mg/mL PFJ-treated human DU145 cells for 24 h as described in the Supporting Information data. An amount of 100  $\mu$ g proteins was loaded on linear pH gradient strip followed by vertical separation on 12.5% SDS polyacrylamide gels as described in Section 2. The gels shown were the representatives of nine pairs of (A) Naïve DU145 cells and (B) PFJ-incubated DU145 cells. The numbers shown on the top of the gel indicated the pH range and those on the left indicated the approximate molecular mass (kDa) determined by Bio-Rad protein markers. The differentially expressed spots were shown by arrows. Three spots were found to be upregulated (spots 1–3) in PFJ-affected cell and eight spots were downregulated (spots A–H).

mass spectrometry. The results of spectrometric analyses were summarized in Table 1 and the matched peptides of each deregulated protein were shown in Supporting Information Table S3. The experimental molecular weight and pI of each protein spot were close to the theoretical values, and the spectrometric protein coverage was entirely above 20%.

The overexpressed proteins (spots 1–3) were identified as heat shock protein 70, lamin A/C (LMNA), and actin-related protein 2 homolog (ARP2). The underexpressed proteins (spots A–H) recognized as valosin containing protein (VCP), human prolidase,  $\alpha$ -enolase (ENO1),  $\beta$ -actin, proteasome subunit  $\alpha$  type 3 (PSMA3), translationally controlled tumor protein (TCTP), mago nashi homolog 2, and ubiquitin conjugating enzyme E2N (UBE2N) (Table 1). Aberrant expression of LMNA is a common feature in a variety of different cancers [23]. Apoptosis is generally preceded by pronounced changes of the actin cytoskeleton. ARP2 is essential for the assembly and maintenance of actin-based structures in the cell [24]. A stronger VCP expression is associated with metastasis and prognosis in prostate cancer [25]. Overexpression of ENO1 has been found in highly tumorigenic or metastatic cells in lung cancer and head/neck cancer [26]. Cytoplasmic  $\beta$ -actin may be correlated to intravasation of cancer cell and thus to invasiveness of tumor cell [27, 28]. The enhanced proteasome activity contributes to tumorigenesis by offering cancer cell with antiapoptotic protection [29]. PFJ could dampen the expression of genes involved in proteasome activity (PSMA3 and UBE2N) to hinder DU145 cell proliferation. TCTP is a novel antiapoptotic protein, which is highly expressed in several cancer cell types including prostate cancer [30–33]. The overall experimental results indicated that the influences of PFJ on the deregulated proteins were in accordance with the inhibitory effects of PFJ on DU145 cells.

### 3.6 Confirmation of differentially expressed proteins by Western blotting

To validate our speculation on the proteomics results, Western immunoblotting was employed to assess the expression of VCP, ENO1,  $\beta$ -actin, and LMNA. These four proteins were chosen as proteins of interest by high-fold alteration and potential relevant characteristics to prostate cancer. Although the deregulation of LMNA and VCP were close to statistically significant, consistent with the proteomics data the results of Western immunoblotting demonstrated that VCP, ENO1 and  $\beta$ -actin were discovered to be downregulated in PFJ-treated DU145 cells whereas LMNA was found to be upregulated (Fig. 4A). Asai et al. [34] reported that VCP is known to be involved in the ubiquitination process of  $\text{I}\kappa\text{B-}\alpha$  (endogenous inhibitor of  $\text{NF-}\kappa\text{B}$ ) and can regulate the activation of  $\text{NF-}\kappa\text{B}$ . Thus Western immunoblotting with the antibody against p65 component of  $\text{NF-}\kappa\text{B}$  was carried out to clarify whether PFJ could impact the activation of  $\text{NF-}\kappa\text{B}$ . Western

**Table 1.** Differentially expressed proteins identified by mass spectrometry<sup>a)</sup>

Spot	Protein identity	Incidence	<i>p</i> -value	Experimental p/MW(kDa)	Theoretical p/MW(kDa)	Matched <sup>b)</sup> peptide number	Coverage (%)	Accession number (NCBI)	Fold
1	Heat shock protein 70	6/9	<i>P</i> < 0.05	5.39/66.62	5.37/70.90	14	37.62	EAW67539	+3.13
2	Lamin A/C	6/9	<i>p</i> = 0.08	6.62/69.5	8.91/87.37	9	14.18	EAW52998	+2.65
3	Actin-related protein 2 homolog	6/9	<i>p</i> < 0.05	6.68/41.07	6.29/44.76	3	10.41	EAW99908	+2.62
A	Valosin containing protein	6/9	<i>p</i> = 0.07	5.07/73.48	5.14/89.32	8	16	AAI21795	−2.33
B	Prolidase	5/9	<i>p</i> = 0.16	5.89/54.14	5.64/54.55	2	9.92	2IW2_A	−3.16
C	α-Enolase	6/9	<i>p</i> < 0.05	6.44/46.60	7.01/47.17	6	20.51	CAA34360	−3.13
D	β-Actin	6/9	<i>p</i> < 0.01	5.16/44.19	5.29/41.74	6	26.67	EAW87341	−3.88
E	Proteasome subunit α type 3	6/9	<i>p</i> < 0.01	5.00/31.40	6.12/24.22	4	17.81	EAW80715	−2.59
F	Translationally controlled tumor protein	6/9	<i>p</i> < 0.05	4.69/24.67	4.84/19.60	3	18.02	P13693	−2.31
G	Protein mago nashi homolog 2	5/9	<i>p</i> < 0.01	5.92/17.69	5.96/17.28	2	20.95	BAB14202	−3.54
H	Ubiquitin conjugating enzyme E2N	7/9	<i>p</i> < 0.01	6.08/17.68	6.13/17.14	2	19.74	BAA11675	−3.3

a) Matched peptide number: Number of peptides matched with protein in MS/MS query. Coverage: Total percentage of amino acid sequence covered by peptides identified by MS/MS analyses.

b) The detail data of MS/MS identification for each peptide are provided in Supporting Information Table S2.

immunoblotting analysis showed that PFJ could decrease the amount of p65 in the cytoplasm of DU145 cell, which along with p50 subunit moves to nucleus to activate the target genes when NF-κB is activated, compared to that in untreated-DU145 cell and also hindered the translocation of p65 into nucleus (Fig. 4B). The aforementioned results implied that PFJ could inhibit the NF-κB activation. Topisirovic et al. [35] found that p53-UBE2N complexes on polysomes can prevent p53 multimerization and render it to become transcriptionally inactive. Activation of c-Jun N-terminal kinase (JNK) disrupts the complex, increasing p53 multimerization and thus leading to p53 activation. Also p53 activation induces the downregulation of UBE2N expression. Since PFJ could decrease UBE2N expression, we hypothesized that JNK was activated and thus induce p53 activity in PFJ-treated DU145 cells. Western immunoblotting with antibody against active JNK (phosphorylated JNK, p-JNK) found that the amount of p-JNK was increased in PFJ-affected DU145 cells, implicating that PFJ could elicit the activation of JNK and thus evoked p53 activity (Fig. 4C).

#### 4 Discussion

Pomegranate has been illustrated to possess anticarcinogenic properties that may suppress various cancers. Many re-

search applications have been made to determine the effects of pomegranate on prostate cancer. They have shown that pomegranate polyphenols can inhibit prostate cancer growth both in vitro and in vivo [5, 9, 15–18]. Moreover, daily consumption of an 8-ounce pomegranate fruit juice following primary treatment of prostate cancer patients can extensively lengthen prostate-specific antigen doubling time [36]. Since PFJ has been demonstrated to possess such effects on cancer, we chose to use a commercially available pomegranate fruit juice (Royal Chef Brand, imported from Republic of Georgia) to facilitate the convenience of patient consumption. We investigated the specific proteins affected by PFJ in prostate cancer cells using gel-based proteomics to shed light on the molecular mechanism underlying cancer intervention of PFJ.

In this research, we found 11 differentially expressed proteins upon treatment of PFJ to DU145 cells with three up-regulated and eight downregulated proteins. Among these dys-regulated proteins, altered regulations of LMNA, VCP, and prolidase were not statistically significant but Western immunoblotting analyses indicated that the expressions of LMNA and VCP were changed upon PFJ treatment.

Among these deregulated proteins, LMNA, localized to the inner surface of the nuclear envelope, is a protein belonging to a family of lamins. They are involved in nuclear stability and providing structural support [37]. It has been found that reduced or even absent expression of LMNA is a common



feature in a variety of different cancers, e.g. prostatic carcinoma, leukemia, and lymphomas etc. [23]. Reduced LMNA expression is also associated with cancer subtypes, cancer aggressiveness, and proliferative activity [38]. Other experiments found this protein was necessary for retinoblastoma protein (Rb) stabilization, and thus a decreased LMNA expression might reflect a decrease in the activity of Rb that is a tumor suppressor protein [39,40]. As LMNA was shown to be overexpressed in PFJ-treated DU145 cells, we suggested that PFJ might have the antitumorigenic characteristics by increasing LMNA expression to enhance Rb activity.

Apoptosis is generally manifest with profound changes of the actin cytoskeleton. ARP2 is essential for the assembly and maintenance of actin-based structures in the cell and localizes in lamellipodia during cell shape alteration prominent in apoptosis [41]. In accordance with DU145 cell apoptosis triggered by PFJ, ARP2 gene expression was altered by PFJ treatment.

VCP is a protein that belongs to the ATPases (AAA) superfamily linked with various cellular activities, including vesicle transport as well as fusion and 26S proteasome function etc. VCP is known to be involved in ubiquitin/proteasome degradation pathway, which has a function in controlling the levels of various cellular proteins and therefore regulates basic cellular processes such as cell-cycle progression, signal transduction, and cell transformation [42]. The enhanced proteasome activity contributes to tumorigenesis by offering cancer cell with antiapoptotic protection and efficient elimination of abnormal proteins. Because of its involvement in the ubiquitin/proteasome degradation pathway, it is identified to promote cell proliferation and decrease cell death in human cancer cells [43]. VCP is revealed to be responsible for some cellular activities such as cell-cycle transition as well as growth control and is postulated to play a crucial role in tumor invasion and metastasis [34]. Tsujimoto et al. [25] reported that a stronger VCP expression in prostate cancer is associated with higher progression and metastasis of prostate cancer. Accordingly, the increased level of VCP is found to cause the activation of nuclear factor- $\kappa$ B signaling, cell proliferation and metastasis [25, 34]. Consistent with the above descriptions, our data indicated that PFJ was able to downregulate the VCP expression and impede the translocation of p65 in prostate cancer cells, suggesting that PFJ might hinder prostate cancer cell growth by lowering the VCP expression to inhibit NF- $\kappa$ B pathway and the proteasome activity. In addition, PFJ could also inhibit the proteasome activity by suppressing the expression of PSMA3 that is a component of 20S proteasome core of 26S proteasome.

UBE2N is a member of E2 ubiquitin-conjugating enzyme family and can activate NF $\kappa$ B pathway that plays a vital role in carcinogenesis and antiapoptosis in a number of cancer types [44]. Consistently, our study showed that PFJ dwindled the expressions of UBE2N and VCP, also a positive regulator of NF- $\kappa$ B pathway, implying that PFJ might impair DU145 cell proliferation via inhibiting NF- $\kappa$ B signaling pathway. The

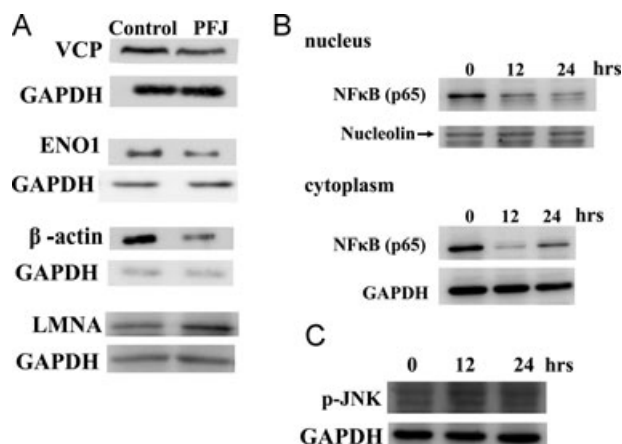


**Figure 4.** Confirmation of the effects of PFJ on the expression levels of LMNA,  $\beta$ -actin, ENO1, VCP, NF $\kappa$ B, and p-JNK by Western immunoblotting. (A) Human DU145 cells were exposed in the presence of 7.5 mg/mL PFJ for 24 h. LMNA,  $\beta$ -actin, ENO1, and VCP in cell lysates were detected by Western immunoblotting as described in Section 2. The blot was the typical data of three independent studies. Control, untreated DU145 cells; PFJ, PFJ-treated cells. (B) Western immunoblotting was used to measure the amount of NF $\kappa$ B/p65 present in the cytoplasm and nucleus. Human DU145 cells were incubated with 7.5 mg/mL PFJ for 0, 12, and 24 h. Nuclear as well as cytoplasmic extracts were isolated as described in the Supporting Information data. The blot was the representative result of three independent investigations. (C) p-JNK in human DU145 cells. Human DU145 cells were treated with 7.5 mg/mL PFJ for 0, 12, and 24 h.

reduced activity of NF- $\kappa$ B cascade in DU145 cell elicited by PFJ was likely to be an important cancer intervention mechanism carried out by pomegranate fruit juice against prostate cancer. Besides, UBE2N regulates p53 activity via manipulating the formation of p53-UBE2N complexes on polysomes by JNK signaling and p53 activation induces the downregulation of UBE2N expression, suggesting the presence of an UBE2N-p53 feedback loop [35]. Moreover, JNK activation is required for mycophenolic acid-induced apoptosis in an insulin-secreting cell [45]. Our study demonstrated that PFJ could attenuate the UBE2N expression and activate JNK, implicating that PFJ might provoke DU145 cell apoptosis via altering UBE2N expression and activating JNK signaling pathway.

$\alpha$ -Enolase is known to be mainly involved in glycolysis, which catalyzes the conversion of 2-phosphoglycerate to phosphoenolpyruvate.  $\alpha$ -Enolase may be an upregulated stress protein in hypoxic situations which tumor cells encounter before angiogenesis, providing protection to cells by increasing anaerobic metabolism [46]. Normal cells increase gene expression of glycolytic enzymes to adapt to environmental stress that is triggered by activation of hypoxic-inducible transcription factor [47]. This cellular process is reversible in normal cells, but not in malignant cells. Tumor cells implement aerobic glycolysis for inefficient energy metabolism known as the Warburg effect, which increases the difficulties

for treatment [48]. Essentially, glycolytic enzymes are commonly upregulated in various cancers. Since ENO1 is one of the target genes of oncogenes Akt and myc [49], which stimulate anaerobic glycolysis directly, it exemplifies that the elevated gene expression of ENO1 is an inevitable consequence during tumorigenesis. Furthermore, a bioinformatics study revealed a correlation between the upregulated expression of ENO1 and tumorigenicity in 18 of 24 types of cancer [50]. Therefore, our results demonstrating the downregulation of ENO1 by treatment of PFJ implicated that PFJ might lower the levels of glycolytic enzymes to interfere with the normal energy production of cancer cell and thus inhibit DU145 cell proliferation.

$\beta$ -Actin belongs to one of human actin isoforms. Specifically,  $\beta$ -actin is a nonmuscle cytoskeletal actin involved in cell motility, structure, and integrity [51]. It was found that an upregulation of  $\beta$ -actin is correlated to increased cell locomotion, particularly in protrusion [52]. Correlation with this, the cytoplasmic  $\beta$ -actin may play an important role in the “ameboidal” type of movement, which is linked with cancer cell intravasation [53]. Moreover, others have supported that  $\beta$ -actin participates in pseudopodial protrusion and invasiveness of tumor cells [54].  $\beta$ -Actin was found to be higher in invasive cells of colon adenocarcinoma rather than in non-invasive ones, further supporting that  $\beta$ -actin may be involved in metastasis [55].  $\beta$ -actin was observed to have the greatest fold of differential expression in our study by being downregulated up to almost fourfold, implying that PFJ might contain the properties that restrain metastasis and invasiveness of prostate cancer cells by the decrease in  $\beta$ -actin expression.

Mago nashi homolog 2 is involved in the mRNA splicing and nonsense-mediated mRNA decay pathway that eliminates mRNAs containing premature translation-termination codons [56]. Chromatography-based proteomics using iTRAQ technique reported by Garbis et al. [57] showed that mago nashi homolog 2 is upregulated in prostate cancer cell. Consistent with the observation by Garbis et al., our study found that PFJ could suppress the expression of mago nashi homolog 2 and thus possibly interfere with the mRNA turnover in prostate cancer cell, which in turn affects tumor cell proliferation.

Prolidase mediates the final step of collagen degradation. It specifically cleaves the imidodipeptide with C-terminal proline or hydroxyproline rich in collagen and recycles proline for collagen resynthesis in the cell [58]. Prolidase serve as a step-limiting role in the metabolism of collagen and regulates the collagen biosynthesis at transcriptional and posttranscriptional level [59]. Collagen is predominantly abundant in extracellular matrix. Successful degradation of extracellular matrix by metalloproteinases is essential for tumor invasion and metastasis. Thus prolidase is associated with tumor invasion and metastasis [60]. Many well-documented evidences also showed that prolidase can provoke the expression of HIF-1  $\alpha$ , VEGF, and HIF-dependent gene product, suggesting that it also is involved in angio-

genesis [60]. In this study, we found that PFJ could decrease prolidase gene expression and therefore might inhibit the invasion capability and the angiogenesis of DU145 cell.

Previous studies demonstrated that pomegranate can inhibit prostate tumor growth [15–18]. These studies attribute pomegranate-induced tumor growth inhibition to the mechanism that pomegranate can evoke CaP cell apoptosis via dys-regulating the expressions of proapoptotic as well as antiapoptotic proteins and deregulating cyclins and cyclin-dependent kinases [15–17]. PE was also found to restrain angiogenesis in CaP through downregulation of VEGF activator, HIF-1 $\alpha$  by transcriptional regulation [18]. Our comparative proteomics data suggested that pomegranate fruit juice could restrain prostate cancer via manipulating the expressions of genes related to apoptosis, metabolic transformation (energy production), ubiquitin/proteasome degradation, NF $\kappa$ B signaling pathway, invasion/metastasis, angiogenesis, and cytoskeleton. Compared to the documented mechanism, in this study we proposed a novel multi-pathway-involved mechanism of PFJ-induced prostate cancer intervention. PFJ was able to (i) induce prostate cancer cell apoptosis by downregulation of TCTP and UBE2N expressions; (ii) restrain prostate cancer cell invasiveness/metastasis by inhibiting the expressions of VCP and prolidase; (iii) impact the activation of NF- $\kappa$ B signaling pathway in prostate cancer cell via the underexpression of VCP and UBE2N; (iv) decrease the proteasome activity in prostate cancer cell by lowering the expressions of VCP and PSMA3; (v) interfere with the metabolic transformation by lowering ENO1 expression; (vi) manipulate the angiogenesis by the downregulation of prolidase; (vii) change the cell morphology through the deregulations of LMNA, ARP2, and  $\beta$ -actin in prostate cancer. This study provided an illustration of significant proteins that interact with molecules present in PFJ, which may cause a beneficial effect whether in preventing or treatment of prostate cancer. Hopefully, our present findings may lead to the development of potential molecular markers for CaP and at the same time, contribute to generating novel ideas for PFJ as chemopreventive and therapeutic technique for prostate cancer.

*The authors would like to thank the National Science Council of Taiwan for financially supporting this research under Contract No. NSC 99–2313-B-218–001-MY3 and the technical services (supports) provided by Proteomics Research Center of the National Yang-Ming University.*

*The authors have declared no conflict of interest.*

## 5 References

- [1] Siegel, R., Ward, E., Brawley, O., Jemal, A., Cancer statistics, 2011. *CA Cancer J. Clin.* 2011, 61, 212–236.
- [2] Cancer Registry Annual report, Bureau of Health Promotion, Department of Health, The Executive Yuan, Taiwan 2008.

- [3] Cancer facts and figures, American Cancer Society, Atlanta 2011.
- [4] Saleem, M., Adhami, V. M., Siddiqui, I. A., Mukhtar, H., Tea beverage in chemoprevention of prostate cancer: a mini-review. *Nutr. Cancer* 2003, *47*, 13–23.
- [5] Parnes, H. L., Thompson, I. M., Ford, L. G., Prevention of hormone-related cancers: prostate cancer. *J. Clin. Oncol.* 2005, *23*, 368–377.
- [6] Mukhtar, H., Ahmad, N., Cancer chemoprevention: future holds in multiple agents. *Toxicol. Appl. Pharmacol.* 1999, *158*, 207–210.
- [7] Surh, Y. J., Cancer chemoprevention with dietary phytochemicals. *Nat. Rev. Cancer* 2003, *3*, 768–780.
- [8] Block, G., Patterson, B., Subar, A., Fruit, vegetables and cancer prevention: a review of the epidemiological evidence. *Nutr. Cancer* 1992, *18*, 1–29.
- [9] Hong, M. Y., Seeram, N. P., Heber, D., Pomegranate polyphenols downregulate expression of androgen synthesizing genes in human prostate cancer cells overexpressing the androgen receptor. *J. Nutr. Biochem.* 2008, *19*, 848–855.
- [10] Gil, M. I., Tomas-Barberan, F. A., Hess-Pierce, B., Holcroft, D. M. et al., Antioxidant activity of pomegranate juice and its relationship with phenolic composition and processing. *J. Agric. Food Chem.* 2000, *48*, 4581–4589.
- [11] Cerda, B., Ceron, J. J., Tomas-Barberan, F. A., Espin, J. C., Repeated oral administration of high doses of pomegranate ellagitannin punicalagin to rats for 37 days is not toxic. *J. Agric. Food Chem.* 2003, *51*, 3493–3501.
- [12] Cerda, B., Llorach, R., Ceron, J. J., Espin, J. C. et al., Evaluation of the bioavailability and metabolism in the rat of punicalagin, an antioxidant polyphenol from pomegranate juice. *Eur. J. Nutr.* 2003, *42*, 18–28.
- [13] Khan, N., Hadi, N., Afaq, F., Syed, D. N. et al., Pomegranate fruit extract inhibits prosurvival pathways in human A549 lung carcinoma cells and tumor growth in athymic nude mice. *Carcinogenesis* 2007, *28*, 163–173.
- [14] Khan, N., Afaq, F., Kweon, M. H., Kim, K. et al., Oral consumption of pomegranate fruit extract inhibits growth and progression of primary lung tumors in mice. *Cancer Res.* 2007, *67*, 3475–3482.
- [15] Malik, A., Afaq, F., Sarfaraz, S., Adhami, V. M. et al., Pomegranate fruit juice for chemoprevention and chemotherapy of prostate cancer. *Proc. Natl. Acad. Sci. USA* 2005, *102*, 14813–14818.
- [16] Rettig, M. B., Heber, D., An, J., Seeram, N. P. et al., Pomegranate extract inhibits androgen-independent prostate cancer growth through a nuclear factor-kappaB-dependent mechanism. *Mol. Cancer Ther.* 2008, *7*, 2662–2671.
- [17] Hong, M. Y., Seeram, N. P., Heber, D., Pomegranate polyphenols down-regulate expression of androgen-synthesizing genes in human prostate cancer cells overexpressing the androgen receptor. *J. Nutr. Biochem.* 2008, *19*, 848–855.
- [18] Sartippour, M. R., Seeram, N. P., Rao, J. Y., Moro, A. et al., Ellagitannin-rich pomegranate extract inhibits angiogenesis in prostate cancer in vitro and in vivo. *Int. J. Oncol.* 2008, *32*, 475–480.
- [19] Forsythe, J. A., Jiang, B. H., Lyer, N. V., Activation of vascular endothelial growth factor gene transcription by hypoxia-inducible growth factor 1. *Mol. Cell Biol.* 1996, *6*, 4604–4613.
- [20] Rasheed, Z., Akhtar, N., Anbazhagan, A. N., Ramamurthy, S. et al., Polyphenol-rich pomegranate fruit extract (POMx) suppresses PMACI-induced expression of pro-inflammatory cytokines by inhibiting the activation of MAP kinases and NF- $\kappa$ B in human KU812 cells. *J. Inflamm.* 2009, *6*, 1–12.
- [21] Celik, I., Temur, A., Isik, I., Hepatoprotective role and antioxidant capacity of pomegranate (*Punica granatum*) flowers infusion against trichloroacetic acid-exposed in rats. *Food and Chem. Toxicol.* 2009, *47*, 145–149.
- [22] Liao, K. A., Tsay, Y. G., Huang, L. C., Huang, H. Y. et al., Search for the tumor-associated proteins of oral squamous cell carcinoma collected in Taiwan using proteomics strategy. *J. Proteome Res.* 2011, *10*, 2347–2358.
- [23] Prokocimer, M., Margalit, A., Gruenbaum, Y., The nuclear lamina and its proposed roles in tumorigenesis: projection on the hematologic malignancies and future targeted therapy. *J. Struct. Biol.* 2006, *155*, 351–360.
- [24] Machesky, L. M., Gould, K. L., The Arp2/3 complex: a multifunctional actin organizer. *Curr. Opin. Cell Biol.* 1999, *11*, 117–121.
- [25] Tsujimoto, Y., Tomita, Y., Hoshida, Y., Kono, T. et al., Elevated expression of valosin containing protein (p97) is associated with poor prognosis of prostate cancer. *Clin. Cancer Res.* 2004, *10*, 3007–3012.
- [26] Liu, K. J., Shih, N. Y., The role of enolase in tissue invasion and metastasis of pathogens and tumor cells. *J. Cancer Mol.* 2007, *3*, 45–48.
- [27] Khatilina, S., Functional specificity of actin isoforms. *Inter. Rev. Cytol.* 2001, *202*, 35–98.
- [28] Le, P. U., Nguyen, T. N., Drolet-Savoie, P., Leclerc, N. et al., Increased  $\beta$ -actin expression in an invasive Moloney sarcoma virus-transformed MDCK cell variant concentrates to the tips of multiple pseudopodia. *Cancer Res.* 1998, *58*, 1631–1635.
- [29] Mani, A., Gelmann, E. P., The ubiquitin-proteasome pathway and its role in cancer. *J. Clin. Oncol.* 2005, *23*, 4776–4789.
- [30] Li, F., Zhang, D., Fujise, K., Characterization of fortilin, a novel antiapoptotic protein. *J. Biol. Chem.* 2001, *276*, 47542–47549.
- [31] Tuynder, M., Susini, L., Prieur, S., Besse, S. et al., Biological models and genes of tumor reversion: cellular reprogramming through tpt1/TCTP and SIAH-1. *Proc. Natl. Acad. Sci. USA* 2002, *99*, 14976–14981.
- [32] Arcuri, F., Papa, S., Carducci, A., Romagnoli, R. et al., Translationally controlled tumor protein (TCTP) in the human prostate and prostate cancer cells: expression, distribution, and calcium binding activity. *Prostate* 2004, *60*, 130–140.
- [33] Gnanasekar, M., Thirugnanam, S., Zheng, G., Chen, A. et al., Gene silencing of translationally controlled tumor protein (TCTP) by siRNA inhibits cell growth and induces apoptosis of human prostate cancer cells. *Int. J. Oncol.* 2009, *34*, 1241–1246.

- [34] Asai, T., Tomita, Y., Nakatsuka, S., Hoshida, Y. et al., VCP (p97) regulates NF $\kappa$ B signaling pathway, which is important for metastasis of osteosarcoma cell line. *Jpn. J. Cancer Res.* 2002, *93*, 296–304.
- [35] Topisirovic, I., Gutierrez, G. J., Chen, M., Appella, E. et al., Control of p53 multimerization by Ubc13 is JNK-regulated. *Proc. Natl. Acad. Sci. USA* 2009, *106*, 12676–12681.
- [36] Pantuck, A. J., Leppert, J. T., Zomorodian, N., Aronson, W. et al., Phase II study of pomegranate juice for men with rising prostate-specific antigen following surgery or radiation for prostate cancer. *Clin. Cancer Res.* 2006, *12*, 4018–4026.
- [37] Ostlund, C., Worman, H. J., Nuclear envelope proteins and neuromuscular diseases. *Muscle Nerve* 2003, *27*, 393–406.
- [38] Broers, J. L., Raymond, Y., Rot, M. K., Kuijpers, H. et al., Nuclear A-type lamins are differentially expressed in human lung cancer subtypes. *Am. J. Pathol.* 1993, *143*, 211–20.
- [39] Nitta, R. T., Jameson, S. A., Kudlow, B. A., Conlan, L. A. et al., Stabilization of the retinoblastoma protein by A-type nuclear lamins is required for INK4A-mediated cell cycle arrest. *Mol. Cell. Biol.* 2006, *26*, 5360–5372.
- [40] Johnson, B. R., Nitta, R. T., Frock, R. L., Mounkes, L. et al., A-type lamins regulate retinoblastoma protein function by promoting subnuclear localization and preventing proteasomal degradation. *Proc. Natl. Acad. Sci. USA* 2004, *29*, 101, 9677–9682.
- [41] de Graauw, M., Le Dévédec, S., Tijdens, I., Smeets, M. B. et al., Proteomic analysis of alternative protein tyrosine phosphorylation in 1,2-dichlorovinyl-cysteine-induced cytotoxicity in primary cultured rat renal proximal tubular cells. *J. Pharmacol. Exp. Ther.* 2007, *322*, 89–100.
- [42] Dai, R. M., Li, C. C., Valosin-containing protein is a multi-ubiquitin chain-targeting factor required in ubiquitin-proteasome degradation. *Nat. Cell Biol.* 2001, *3*, 740–744.
- [43] Dou, Q. P., Smith, D. M., Daniel, K. G., Kazi, A., Interruption of tumor cell cycle progression through proteasome inhibition: implications for cancer therapy. *Prog. Cell Cycle Res.* 2003, *5*, 441–446.
- [44] Deng, L., Wang, C., Spencer, E., Yang, L. et al., Activation of the I $\kappa$ B kinase complex by TRAF6 requires a dimeric ubiquitin-conjugating enzyme complex and a unique polyubiquitin chain. *Cell* 2000, *103*, 351–361.
- [45] Park, Y. J., Ahn, H. J., Chang, H. K., Kim, J. Y. et al., The RhoGDI- $\alpha$ /JNK signaling pathway plays a significant role in mycophenolic acid-induced apoptosis in an insulin-secreting cell line. *Cell Signal* 2009, *21*, 356–364.
- [46] Aaronson, R. M., Graven, K. K., Tucci, M., McDonald, R. J. et al., Non-neuronal enolase is an endothelial hypoxic stress protein. *J. Biol. Chem.* 1995, *270*, 27752–27757.
- [47] Semenza, G. L., Jiang, B. H., Leung, S. W., Passantino, R. et al., Hypoxia response elements in the aldolase A, enolase 1, and lactate dehydrogenase A gene promoters contain essential binding sites for hypoxia-inducible 1. *J. Biol. Chem.* 1996, *271*, 32529–32537.
- [48] Tennant, D. A., Durán, R. V., Boulahbel, H., Gottlieb, E., Metabolic transformation in cancer. *Carcinogenesis* 2009, *30*, 1269–1280.
- [49] Kim, J. W., Zeller, K. I., Wang, Y., Jegga, A. G. et al., Evaluation of myc E-box phylogenetic footprints in glycolytic genes by chromatin immunoprecipitation assays. *Mol. Cell. Biol.* 2004, *24*, 5923–5936.
- [50] Altenberg, B., Greulich, K. O., Genes of glycolysis are ubiquitously overexpressed in 24 cancer classes. *Genomics* 2004, *84*, 1014–1020.
- [51] Vandekerckhove, J., Weber, K., At least six different actins are expressed in a higher mammal: an analysis based on the aminoacids sequence of the amino-terminaltryptic peptide. *J. Biol. Chem.* 1978, *126*, 783–802.
- [52] Peckham, M., Miller, G., Wells, C., Zicha, D. et al., Specific changes to the mechanism of cell locomotion induced by overexpression of  $\beta$  actin. *J. Cell Sci.* 2001, *114*, 1367–1377.
- [53] Khatilina, S., Functional specificity of actin isoforms. *Inter. Rev. Cytol.* 2001, *202*, 35–98.
- [54] Le, P. U., Nguyen, T. N., Drolet-Savoie, P., Leclerc, N. et al., Increased  $\beta$ -actin expression in an invasive Moloney sarcoma virus-transformed MDCK cell variant concentrates to the tips of multiple pseudopodia. *Cancer Res.* 1998, *58*, 1631–1635.
- [55] Nowak, D., Krawczenko, A., Duś, D., Malicka-Błaszkiwicz, M., Actin in human colon adenocarcinoma cells with different metastatic potential. *Acta Biochim. Polon.* 2002, *49*, 823–828.
- [56] Palacios, I. M., Gatfield, D., St Johnston, D., Izaurralde, E., An eIF4AIII-containing complex required for mRNA localization and nonsense-mediated mRNA decay. *Nature* 2004, *427*, 753–757.
- [57] Garbis, S. D., Tyritzis, S. I., Roumeliotis, T., Zerefos, P., Search for potential markers for prostate cancer diagnosis, prognosis and treatment in clinical tissue specimens using amine-specific isobaric tagging (iTRAQ) with two-dimensional liquid chromatography and tandem mass spectrometry. *J. Proteome Res.* 2008, *7*, 3146–3158.
- [58] Endo, F., Tanoue, A., Nakai, H., Hata, A. et al., Primary structure and gene localization of human prolidase. *J. Biol. Chem.* 1989, *264*, 4476–4481.
- [59] Surazynski, A., Miltyk, W., Palka, J., Phang, J. M., Prolidase-dependent regulation of collagen biosynthesis. *Amino Acids* 2008, *35*, 731–738.
- [60] Surazynski, A., Donald, S. P., Cooper, S. K., Whiteside, M. A., Extracellular matrix and HIF-1 signaling: the role of prolidase. *Int. J. Cancer* 2008, *122*, 1435–1440.